



Research Article

# Adsorption studies of packed bed column for the removal of dyes using amine functionalized radiation induced grafted fiber

Sarala Selambakkannu<sup>1</sup>  · Nor Azillah Fatimah Othman<sup>1</sup> · Khomsaton Abu Bakar<sup>1</sup> · Zulhairun Abdul Karim<sup>2</sup>

© Springer Nature Switzerland AG 2019

## Abstract

In this paper, the adsorption performance of packed bed column with amine functionalized radiation-induced grafted fibers (AFF) for the removal of acid blue 80 (AB 80) was investigated. Pretreated banana fibers were grafted with glycidyl methacrylate (GMA) with the assistance of electron beam irradiation and subsequently functionalized with imidazole, which was used as the precursor of anionic dye adsorption. The effect of flow rate, bed height and inlet concentration on the breakthrough curves were analyzed in terms of AFF adsorption performance. The experiment revealed that the increase in bed height and inlet concentration promoted the adsorption efficacy, whereas reduction was observed when the flow rate increased. The highest bed capacity obtained was 194.45 mg/g at adsorption condition of 5 ml/min flow rate, 100 mg/l inlet concentration and 50 mm of bed height. In order to determine the optimum operational parameters, the data were collected via the experiment fitted into Yoon and Nelson, and Thomas and Bed Depth Service Time (BDST) mathematical models. At various conditions, Thomas model closely defined the behaviors of the breakthrough curves. The maximum adsorption capacity calculated from Yoon–Nelson and Thomas models increased with the increase in flow rate and inlet concentration. However, a reduction was observed with the increase in bed height. Meanwhile, the BDST model exhibited good agreement with the experimental data as well as high correlation coefficient value  $r^2 \sim 0.99$ , which indicated the validity of BDST model for the column adsorption system with AFF. The experimental results attained had suggested that developed AFF is quite effective as a biosorbent for the removal of the dyes.

**Keywords** Acid blue 80 · Electron beam · Glycidyl methacrylate · Flow rate · Bed height and inlet concentration

## 1 Introduction

One of the basic roles played by water is the integrity maintenance of the natural environment. Water also plays a vital role as a key factor in economic and social development. Apart from the adequate availability of water assets, pollution of water resources related to water also requires serious attention. Furthermore, water pollution threatens the equilibrium and conservation of natural ecosystem. A substantial volume of waste water is generated by the various types of industries such as food, paper, plastics and textile. Emission of synthetic dyes from textile production

activities are identified as the main pollutant found on water resources. Approximately 12% of synthetic dye loss is expected during textile industries manufacturing and processing operations [1]. Dye compounds are made of two main components, namely chromophores and auxochromes, which are responsible for the dye color and dye intensity, respectively [2]. Stability of dye compounds is endowed by its synthetic and complex aromatic structure, which inhibits biodegradation [3]. This leads to suppression of photosynthetic activities in aquatic habitats by deterring the penetration of sunlight [4].

✉ Sarala Selambakkannu, sarala@nuclearmalaysia.gov.my | <sup>1</sup>Malaysian Nuclear Agency, Radiation Processing Technology, Bangi, 43000 Kajang, Selangor, Malaysia. <sup>2</sup>Faculty of Engineering, Advanced Membrane Technology Research Centre (AMTEC), School of Chemical and Energy Engineering, Universiti Teknologi Malaysia, 81310 Skudai, Johor, Malaysia.



SN Applied Sciences (2019) 1:175 | <https://doi.org/10.1007/s42452-019-0184-2>

Received: 19 November 2018 / Accepted: 16 January 2019 / Published online: 22 January 2019

The complex structures and synthetic nature of dyes imposes difficulties in treating textile effluent by conventional processes. The common techniques that are practiced are mostly expensive and ineffective on the removal of a wide range of dyes that are present in textile effluents [5]. Some of the dedicated common techniques in practice for the removal of pollutants from wastewater are filtration, ion exchange, precipitation, evaporation, membrane separation, and coagulation-flocculation. All these methods are associated with complex procedures and economically infeasible, which makes them inappropriate for practical use. Adsorption technique appears to be the most efficient method for the removal of dyes from wastewater. Adsorption process offers simplicity in terms of the design, flexibility and impose high selectivity towards targeted pollutants [6]. This method is economical as the adsorbents are re-generable and also non-generable secondary sludge [7].

The dispute about some common adsorbent such as activated carbon is involving high operational cost and challenging for regeneration [8]. In this scenario, potentially low-cost adsorbents are the most appropriate choice. Low cost adsorbent developed from agricultural waste leads to new biosorption pathways. Biosorption is the removal of metals, compounds or particulates from aqueous solution by inactive, non-living biomass [9]. This method also appears to be eco-friendly. Banana fiber, an agricultural waste, had been used as the precursor for the adsorption of dye in this study. The banana stalk would be excluded as waste which serves no purpose after the fruits have been harvested [10]. Hence, every attempt to reuse the banana fibers will be beneficial. The banana fiber was grafted with GMA by using radiation graft polymerization technique (RIGP) and subsequently functionalized with IMI. Radiation induced surface modification via grafting co-polymerization technique offers benefits economically by indefinite efficiency without chemical initiation [11]. The adsorption of dye was executed by column mode in this experiment.

Most of the adsorption studies were performed on batch mode which is unfeasible for large scale or for continuous flow [12]. Furthermore, batch adsorption is more applicable for laboratory scale experiments and inappropriate for field application. Moreover, the batch equilibrium adsorption experiment helps to determine the maximum adsorption capacity and also measure the efficiency of adsorption for removing targeted adsorbate. Adsorption data obtained from batch experiments is invalid for certain treatment, especially on those involving column operations as the contact time is inadequate to reach adsorption equilibrium [13]. Thus, fixed-bed column study is needed for continuous flow sorption for determination of basic bed operation data such as operational life span

and regeneration time [14]. Experimental breakthrough curve can also be determined using fixed bed sorption system. The fixed bed sorption system establishes practical applicability of the sorbent in continuous mode, which is also suitable for large scale of wastewater volumes. The removal of dyes by adsorption using column system is very beneficial due to adjustment of column system towards versatile processes, less reagent controlling and low operational cost [15].

Leaching of dye particles into soil or groundwater via rapid industrialization activities could lead to severe contamination and a precised model is essential to estimate the sorption process quantitatively. Thus, in this work, banana fibers had been developed as biosorbent, AFF via pre-radiation grafting technique in order to imitate the natural surroundings for the sorption of dye particles in continuous mode. This had been never emphasized in any studies before. Versatility and sustainability of the developed novel bioadsorbent in continuous adsorption mode is crucial to be explored in order to estimate the total performance. The main objective of this study is to assess the performance of AFF on the adsorption of acid blue 80 (AB 80) dye in aqueous solution of active flow system. The effect of flow rate, bed height and inlet concentration on the breakthrough curves were analyzed in terms of AFF adsorption performance.

## 2 Experimental

### 2.1 Materials

Innovative Pultrusion Sdn. Bhd. (Malaysia) supplied the polymer trunk derived from lignocellulosic banana fibers that were used in this study. Glycidyl methacrylate (GMA, 97%), polyoxyethylene sorbitol ester (TWEEN 20), imidazole (IMI, 99%, 68.08 g/mol) and Isopropanol (IPA, 99.7%) were procured from Sigma. The AB80 dye solution for column adsorption studies were prepared from AB80 dye powder manufactured by Sigma-Aldrich. The chemical structure of AB 80 dyes is shown in Fig. 1. All chemicals were of analytical grade.

### 2.2 Methods

#### 2.2.1 Irradiation-induced polymer grafting

Prior to grafting, the banana fibers were partially delignified using  $\text{NaClO}_2$  via acid chlorite method defined elsewhere [10]. Fixed amount of delignified fibers were packed in polyethylene zipper bag which was subsequently purged with nitrogen ( $\text{N}_2$ ) in order to replace the existing air inside the bag. The packed samples were irradiated

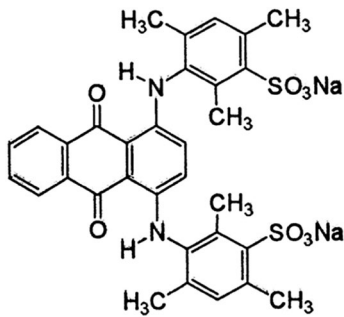


Fig. 1 Chemical structure of acid blue 80 (AB 80)

with conveyer-type electron beam accelerator (EPS 3000 Nissin High Voltage, Japan) at dry ice temperature. Technical conditions of EPS 3000 are; accelerator voltage: 0.5–3.0 MeV, beam current: 1–30 mA, max beam power: 90 kW and conveyor speed: 1–20 m/min. The optimum radiation condition for fiber sample was 30 kGy electron, 2 MeV voltage, and 10 mA current. The irradiated sample was shifted into a glass ampoule and vacuumed for 1 min. Emulsified monomer solution comprised of GMA/TWEEN 20 (3:1 ratio) was transferred into the glass ampoule containing the irradiated fibers. The glass ampoule was placed in a 40 °C water bath for 1.5 h for grafting reaction to occur. Finally, the polymer-grafted banana fibers were dried in an oven at 50 °C overnight.

The grafting yield,  $D_g$  %, was calculated as:

$$D_g\% = \frac{W_g - W_o}{W_o} \times 100\% \quad (1)$$

where  $W_o$  and  $W_g$  denote the mass of the sample before and after grafting process, respectively.

### 2.2.2 Polymer-graft functionalization

30 vol.% IMI in isopropanol solution in total volume of 60 ml was mixed with 0.5 g of grafted fibers and subsequently placed in water bath at 60 °C for duration of 1.5 h. During this duration, bond cleavage of epoxy group on GMA occurs in order to form a bond with IMI. The functionalized fibers were washed with ultrapure water to eliminate the excessive reactants followed by drying in an oven at 50 °C overnight. The amine group density, AD (mmol/g), was calculated by:

$$AD = \frac{Z_i - Z_o/Z_o}{M} \times 1000 \quad (2)$$

where  $Z_i$  and  $Z_o$  denote the mass of the fiber before and after functionalization, respectively, and  $M$  is the molecular weight of the amine.

### 2.2.3 Characterization

**2.2.3.1 FE-SEM analysis** The Field Emission-Scanning Electron Microscope (FE-SEM) analysis was carried out with Carl Zeiss Ultra 55 model. Beam voltage and beam current used was 10 kV and 10 micro amps, respectively. Resolution of 10 nm was used, with magnifications of 500X. The fiber samples were coated with platinum before imaging.

**2.2.3.2 FTIR imaging analysis** GMA-grafted fibers, AFF and dye loaded fibers were analyzed with Fourier Transformed Infrared (FTIR) imaging system using Cary 620 spectrometer (Agilent) in ATR mode via Focal Plane Array (Mapping) technique. FTIR spectra were scanned in the range from 600 to 4000  $\text{cm}^{-1}$ , with a resolution of 4  $\text{cm}^{-1}$  and averaged over 32 scans. IR Field of view and IR pixel view were carried out at 70  $\mu\text{m} \times 70 \mu\text{m}$  and 1.1  $\mu\text{m} \times 1.1 \mu\text{m}$ , respectively.

### 2.2.4 Column setup

The packed bed column experiment was performed in a glass column with an internal diameter of 1.5 cm and a length of 20 cm which connected to peristaltic pump with flow rates up to 20 ml/min and pressures up to 50 psi. A constant amount of glass wool was placed on the bottom and top of the column to provide sustainable support for AFF and also to prevent the adsorbent to be pulled out with outflow. The entire adsorption experiment was conducted on the direction of flow from bottom to top to prevent the influence of gravity on adsorbate flow. No pH adjustment was performed on AB80 dye solution. Effluents were collected at the top of the column at pre-determined time intervals. The initial and residual concentration of AB80 dye in the outlet was analyzed using HACH UV/Vis spectrophotometer (DR 5000) at 625 nm.

### 2.2.5 Column experiments

The effect of flow rate, bed height and inlet concentration on the breakthrough curves were analyzed in terms of AFF adsorption performance. All the column experiments were replicated three times.

**2.2.5.1 Effect of flow rate** The predetermined flow rates were 5, 10, 15 and 20 ml/min to examine the effect on the adsorption performance. The bed height and inlet concentration were kept constant at about 5 cm and 100 ppm, respectively.

**2.2.5.2 Effect of bed height** The predetermined bed heights were 5.0, 7.5 and 10.0 cm to examine the effect

on the adsorption performance. The flow rate and inlet concentration were kept constant at about 10 ml/min and 100 ppm, respectively.

**2.2.5.3 Effect of initial inlet concentration** The predetermined initial inlet concentrations were 50.0, 100.0, 150.0 and 200.0 ppm to examine the effect on the adsorption performance. The bed height and flow rate were kept constant at about 5.0 cm and 10 ml/ml, respectively.

**2.2.6 Mathematical description**

Breakthrough curve derived from plot of  $C_i/C_o$  versus  $t$  was used to evaluate the AFF adsorption performance, where  $C_i$  and  $C_o$  represent the outlet and inlet concentration of AB80 dye concentration in mg/l, respectively. Previous studies had recommended that evaluation of process and the dynamic response of an adsorption column is vital [5, 16]. Total uptake of AB80 dyes by AFF in the column,  $q_{total}$  (mg), for the determined inlet concentration and flow rate were represented by the area under the plot of the adsorbed AB80 concentration,  $C_{ad}$  ( $C_o - C_t$ ), mg/l versus  $t$ , whereby  $C_o$  and  $C_t$  are inlet and outlet concentration, respectively. Equation (3) shows the calculation of experimental uptake capacity,  $q_{e(exp)}$ , mg/g where  $X$ , g denote the dry weight of AFF packed in column.

$$q_{e(exp)} = \frac{q_{total}}{X} \tag{3}$$

The total amount of AB80 ( $W_{total}$ ) added to the column (mg) is calculated via Eq. (4).

$$W_{total} = \frac{C_o Q t_{total}}{1000} \tag{4}$$

The total AB80 removal in % is calculated by Eq. (5)

$$\%removal = \frac{q_{e(exp)}}{W_{total}} \times 100 \tag{5}$$

**2.2.6.1 Yoon and Nelson model** Yoon and Nelson model functions based on the theory that a decrease in the rate of adsorption probability for every adsorbate molecule is proportionate to the probability of adsorbate adsorption and breakthrough onto the adsorbent [5]. This model is less complex in comparison to others as it does not require details of characteristics of adsorbate, the type of adsorbent, and the physical properties of the adsorption. The Yoon and Nelson Eq. (6) is expressed as below.

$$\frac{C_t}{C_o - C_t} = \exp(k_{YN}t - \tau k_{YN}) \tag{6}$$

The plot of Yoon and Nelson model consists of  $C_t/(C_o - C_t)$  versus sampling time ( $t$ ) as shown in Eq. (6) above. Nonlinear regressive model was used to obtain parameters  $k_{YN}$  and  $\tau$  [17].

**2.2.6.2 Thomas model** Thomas model is used to determine the maximum capacity of an adsorbent. The maximum solid phase concentration of the adsorbate, AB 80 dye, onto the adsorbent and adsorption rate constant were determined via the data obtained from continuous mode studies in column using kinetic model developed by Thomas [18]. Model developed by Thomas model is widely used in column performance theory. The expression by Thomas model for an adsorption column is shown in Eq. (7).

$$\ln\left(\frac{C_o}{C_i} - 1\right) = \frac{k_{Th}q_o w}{Q} - k_{Th}C_o t \tag{7}$$

where  $k_{Th}$  represents Thomas model constant ( $ml\ min^{-1}\ mg^{-1}$ ),  $q_o$  is the equilibrium adsorption amount of dye, AB 80 on adsorbent ( $mg\ g^{-1}$ ),  $w$  is the mass of the adsorbent (g) and  $Q$  is the flow rate ( $ml\ min^{-1}$ ).

**2.2.6.3 Bed depth service time (BDST) model** The prompt prediction of an adsorbent performance in fixed-bed analysis is possible by using BDST, a simple semi-empirical model. Based on BDST model, adsorption rate is controlled by surface reaction between adsorbate and the idle capacity of the adsorbent [19]. The relationship between bed depth ( $Z$ ) of the fixed-bed column and service time ( $t$ ) can be predicted using BDST model. The linear relationship between bed depth ( $Z$ ) and service time is expressed in Eq. (8).

$$t = \frac{N'_o}{C_o F} Z - \frac{1}{k_a C_o} \ln\left(\frac{C_o}{C_i} - 1\right) \tag{8}$$

where  $N'_o$  represents the adsorption capacity derived from BDST model ( $mg\ l^{-1}$ ) and  $k_a$  is the rate constant in BDST model ( $l\ mg^{-1}\ min^{-1}$ ).

Simplified version of BDST model is expressed in Eq. (9) below.

$$t = aZ - b \tag{9}$$

where  $a$  ( $min\ cm^{-1}$ ) and  $b$  ( $min$ ) are the first and second terms of Eq. (9) exhibited above.

**3 Results and discussion**

**3.1 Cross section WITH FE-SEM**

Figure 2 displays the FESEM cross section view for GMA grafted, AFF and dye loaded fibers. The micrographs clearly illustrate hollow-centered banana trunk fibers



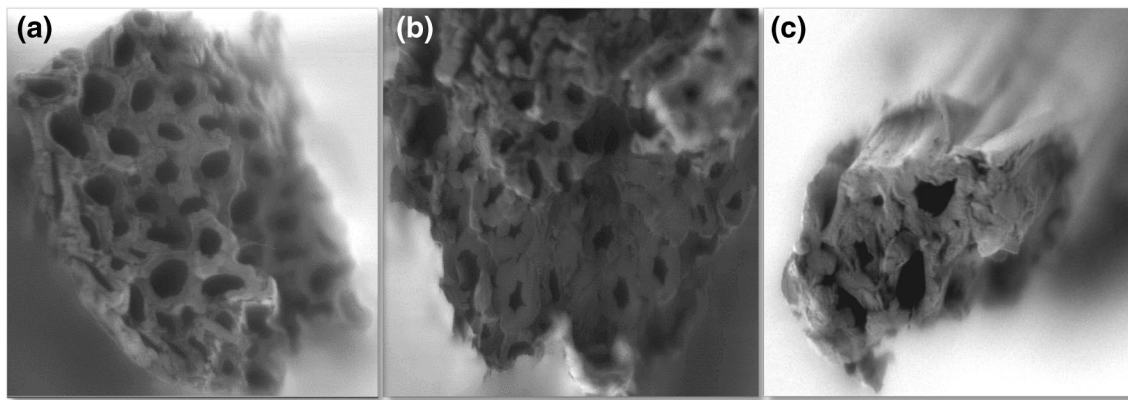


**Fig. 2** FESEM cross section images of hollow-centered banana trunk fiber for **a** GMA grafted fibers, **b** AFF and **c** Dye loaded fibers with magnification of  $\times 500$

with decrease in diameter after functionalization and dye adsorption process. After functionalization process, the diameter of the microfibrils decreases very obviously, evidenced by the incorporation of IMI onto GMA grafted fibers. The diameter of microfibrils grew even smaller after adsorption of dye onto amine functionalized fibers due to loading of large dye molecules onto fibers surface. The average of total surface diameter measured as multifilament was around  $42.24\ \mu\text{m}$ ,  $37.40\ \mu\text{m}$  and  $31.22\ \mu\text{m}$  for GMA grafted fibers, AFF and dye loaded fibers, respectively. The total diameter of multifilament shows reduction after functionalization and adsorption process. This result suggest that the hollow centered fibers shrink with some chemical and physical processes. This observation is in agreement with water content analysis of all three GMA grafted fibers, AFF and dye loaded fibers. The water uptake capacity of GMA grafted fibers are 97.14%, which reduces to 88.45% after functionalization with IMI. Meanwhile, the water uptake capacity of dye loaded fiber is 20.74%. This observation indicates that the functionalization and adsorption process also take place throughout the entire fiber inner surface.

### 3.2 FTIR imaging

The GMA-grafted fibers, AFF and dye loaded fibers were subjected to FTIR imaging analysis and the result obtained is shown in Fig. 3. GMA-grafted fibers exhibit common stretching for lignocellulosic fibers at  $\text{C}=\text{C}$  at  $1632\ \text{cm}^{-1}$ ,  $\text{C}-\text{O}$  stretching of cellulose at  $1016\ \text{cm}^{-1}$  and additional stretching were found at  $1732\ \text{cm}^{-1}$  and  $1040\ \text{cm}^{-1}$  assigned for  $\text{C}=\text{O}$  and  $\text{C}-\text{O}$  stretching vibration, which originates from  $-\text{COO}-$  ester group of GMA. Meantime, both AFF and dye loaded fibers display the common stretching for lignocellulosic fibers and additional stretching attributed by grafting of GMA. Additional stretching found at

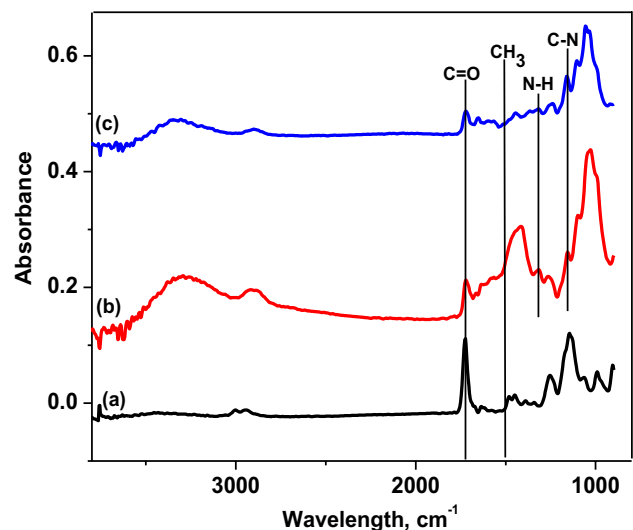


**Fig. 3** FTIR spectra for (a) GMA-grafted fiber (100% grafting yield), (b) AFF (2.00 mmol/g); and (c) Dye loaded fibers (2.00 mmol/g)

$1318\ \text{cm}^{-1}$  and  $1162\ \text{cm}^{-1}$  are assigned for  $\text{N}-\text{H}$  and  $\text{C}-\text{N}$  stretching vibration onto both AFF and dye loaded fibers, respectively. This observation supports the claim of incorporation of imidazole onto GMA-grafted fibers via functionalization process. The peak intensity of common stretching for lignocellulosic fibers, additional stretching attributed by grafting of GMA and functionalization with IMI reduces quite significantly after dye adsorption process. After mass loading of dye molecules onto AFF, the detection of functional groups become difficult, which correspond to weak signal.

Furthermore, the FTIR spectrum obtained is in agreement with FTIR chemical imaging of each sample with focal plane array (FPA) detector at targeted stretching vibration as shown in Fig. 4. Image scanning was carried

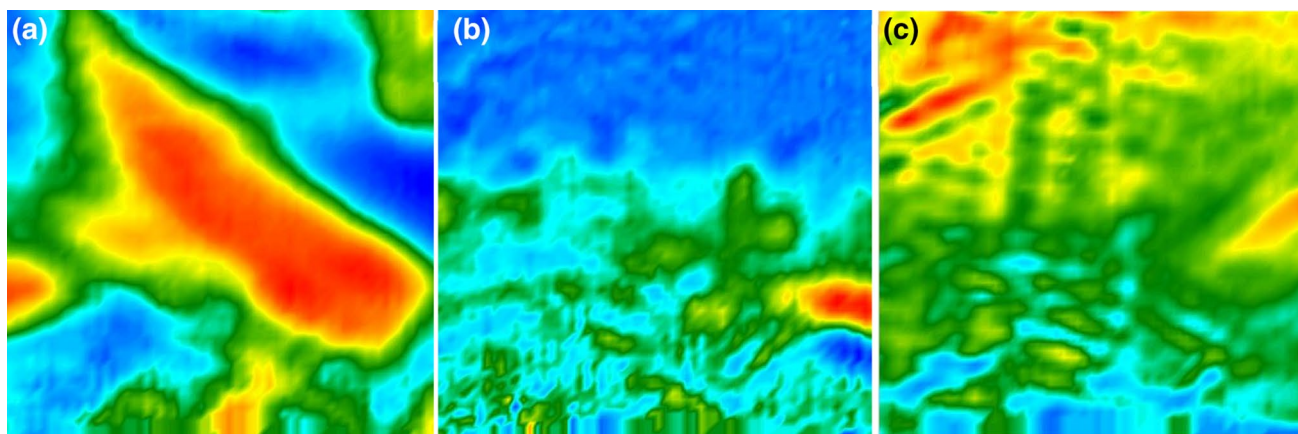


**Fig. 4** FTIR chemical imaging with focal plane array (FPA) detector for **a** GMA-grafted fiber (100% grafting yield), **b** AFF (2.00 mmol/g); and **c** Dye loaded fibers (2.00 mmol/g)

out at stretching vibration of  $C=O$  at  $1732\text{ cm}^{-1}$  onto GMA-grafted fibers. The image attained shows localized high density of carbonyl group, which approves the grafting of GMA with yield of 100%. The image scanned for AFF shows more like smearing type image with very low localized concentration for  $N-H$  group at stretching vibration of  $1318\text{ cm}^{-1}$ . This may be attributed to very low concentration of amine functionalized with GMA, which was around  $2.00\text{ mmol/g}$ . Image scanning was done at a stretching vibration of  $1049\text{ cm}^{-1}$  onto dye loaded samples. Smearing type image with average level of localized concentration of the dye were observed. The grafting and functionalization occur onto the fibers asymmetrically. Thus, the adsorption of dyes also takes place in the same manner.

### 3.3 Column performance

The effect of bed height, flow rate and initial inlet concentration onto the breakthrough curve shape in terms of column performance had been evaluated in this study.

#### 3.3.1 Effect of bed height

The effect of bed height onto breakthrough curve at 50, 75 and 100 mm with fixed inlet initial concentration of  $100\text{ mg/l}$  and flow rate of  $10\text{ ml/min}$  were tested in this study. The result obtained is exhibited in Fig. 5. As the bed height increases, increase in breakthrough time and decrease in the breakthrough slope curve were observed. This observation suggested that rapid mass transfer had taken place. The experimental breakthrough

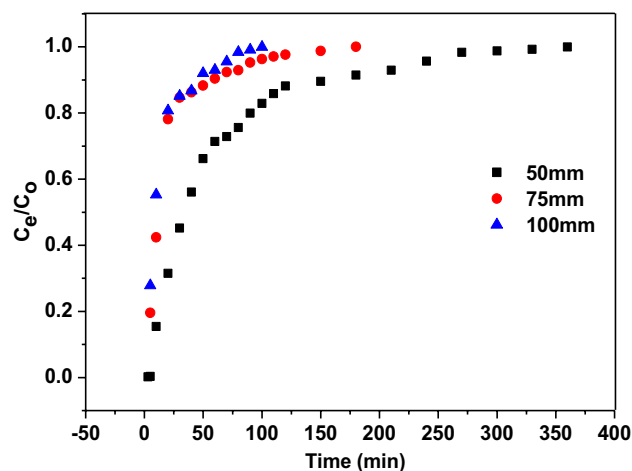


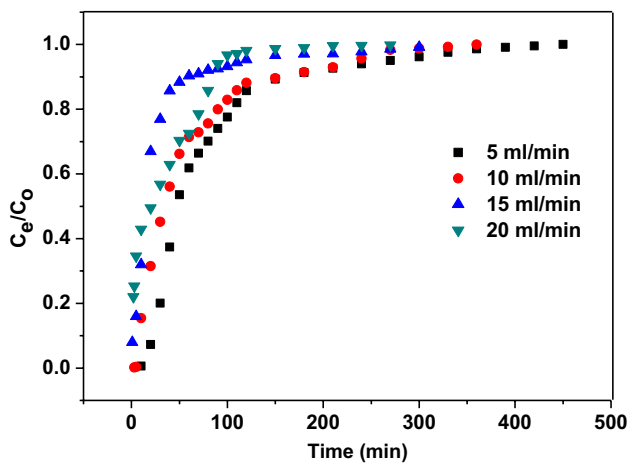
**Fig. 5** Breakthrough curves of AB 80 removal by AFF packed in columns at different bed heights ( $C_0 = 100\text{ mg/l}$ ,  $Q = 10\text{ ml/min}$ )

curve obtained in this study does not follow ideal adsorption system with characteristic 'S' shape profile. The 'S' shape profile is only applicable for adsorbate with small molecular diameters and simple structures and AB 80 is a complex structured molecule [20].

Table 1 below displays adsorption data which comprises AB 81 uptake and dye removal percentage. Dye removal percentage increases from 21.75% to 89.43% when the bed height increases from 50 mm to 100 mm. This observation is supported by total weight of AB 80 adsorbed by AFF, which increases from 235.22 mg to 409.43 mg when the bed height increases from 50 mm to 100 mm. As the bed height increases, surface area of the adsorbent increases as well, which provides more binding sites for the adsorption to occur [16].

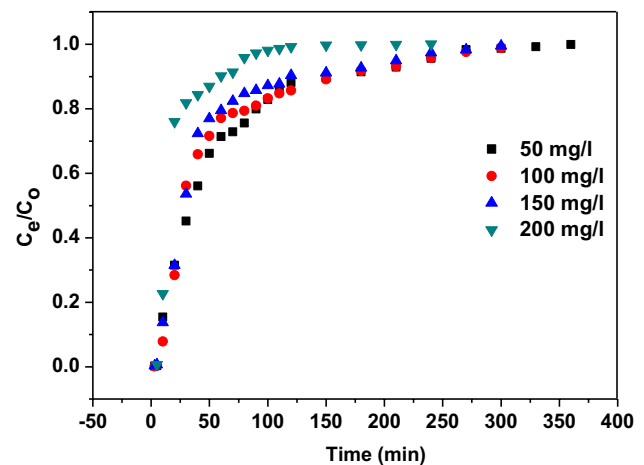
**Table 1** Experimental data of the column parameters determined at various initial inlet concentrations of the AB 80 solution at room temperature

Co (mg/L)	Q (ml/min)	Z (mm)	$q_{\text{total}}$ (mg)	$q_{\text{eq(exp)}}$ (mg g <sup>-1</sup> )	$W_{\text{total}}$ (mg)	% removal
50	10	50	255.84	124.31	158.43	78.46
100	10	50	300.38	130.99	391.07	33.49
150	10	50	313.45	155.1	476.25	32.57
200	10	50	330.51	159.13	597.6	26.63
100	5	50	373.19	194.45	251.93	77.18
100	15	50	270.56	122.06	497.48	24.53
100	20	50	235.22	120.18	552.20	21.75
100	10	75	358.23	104.14	195.84	53.17
100	10	100	409.43	104.9	108.18	96.97

**Fig. 6** Breakthrough curves of AB 80 removal by AFF packed in columns at different flow rate ( $C_0 = 100$  mg/l,  $Z = 50$  mm)

### 3.3.2 Effect of flow rate

The effect of varying flow rate (5, 10, 15 and 20 ml/min) breakthrough curves were investigated whereby bed height of 50 mm and an initial inlet concentration of AB 80 of 100 mg/l are kept constant. The results obtained are displayed in Fig. 6 and Table 1. The breakthrough takes place faster at higher flow rate. The highest removal percentage of AB 80, 77.18% was obtained at lowest flow rate of 5 ml/min and the experimental adsorption capacity of AB 80 was around 194.45 mg/g. The flow rate was inversely proportional to breakthrough time. As the flow rate increases, decrease in breakthrough time was clearly observed. At lower flow rate of inlet AB 80, AFF had greater contact time with dye, which corresponds to higher removal of AB 80 dye in column. Slope of the breakthrough curve and adsorption capacity obtained at different flow rate is explained by basic mass transfer fundamentals. At higher flow rate, the rate of mass transfer increases as the amount of dye adsorbed onto unit bed height is increased with increasing flow rate leading towards faster saturation instantly [21].

**Fig. 7** Breakthrough curves of AB 80 removal by AFF packed in columns at different initial inlet concentration ( $Q = 10$  ml/min,  $Z = 50$  mm)

### 3.3.3 Effect of initial inlet concentration

Four different initial feed concentrations (50, 100, 150 and 200 mg/l) of AB 80 were used to evaluate the effect of initial inlet concentration onto breakthrough curves. The bed height and flow rate were kept constant to 50 mm and 10 ml/min, respectively. The results obtained are shown in Fig. 7 and Table 1. Reduction in breakthrough time was observed as the initial inlet concentration increases. At lower initial inlet concentration, breakthrough occurs at slower rate with dispersed breakthrough curve [5]. The removal percentage reduces from 78.46% to 26.63% as the initial inlet concentration increases from 50 mg/l to 200 mg/l. Meanwhile, the experimental adsorption capacity of AB 80 increases from 255.84 to 330.51 as the initial inlet concentration increases from 50 mg/l to 200 mg/l. Slow transportation of AB 80 dye onto AFF, which is packed inside the column during low initial inlet concentration, is responsible for reduction in diffusion coefficient and mass transfer driving force [22].

### 3.4 Breakthrough curve models

Yoon and Nelson and Thomas models were used to define fixed-bed column behavior in terms of kinetic model to estimate the breakthrough curves.

#### 3.4.1 Yoon and Nelson model

Yoon and Nelson model was applied to examine the breakthrough behavior of AB 80 dye onto AFF which was packed into the column. The rate constant,  $k_{YN}$  and time required to attain 50% of AB 80 breakthrough,  $\zeta$  obtained via experiment is listed in Table 2. The rate constant values,  $k_{YN}$  decrease as the initial inlet concentration of AB 80 dye increases. Meanwhile, increase in rate constant values,  $k_{YN}$  was observed as the flow rate of the AB 80 dye increases. The  $\zeta$  values obtained shows ascending trend with increase in the initial inlet concentration of AB 80 dye. On the other hand, the  $\zeta$  values obtained show descending trend with increase in flow rate of AB 80 dye. The values of  $\zeta$  increases and rate constant value,  $k_{YN}$ , decreases as the bed height increases. The comparison of the experimental curve and predicted curves according to the Yoon and Nelson model are displayed in Fig. 8. The experimental breakthrough curves were incompatible with predicted Yoon–Nelson model curve. Thus, significant deviation was observed between the experimental and predicted values using the Yoon–Nelson model [5].

#### 3.4.2 Thomas model

The rate constant,  $k_{Th}$ , and  $q_0$  values were determined by using linearized form of the Thomas model,  $\ln(C_0/C_i - 1)$  versus  $t$  plot. The Thomas parameters along with liner regression coefficients ( $R^2$ ) obtained via different experimental parameters are presented in Table 3. A comparison between the experimental data and the predicted breakthrough curves at 200 ppm of initial

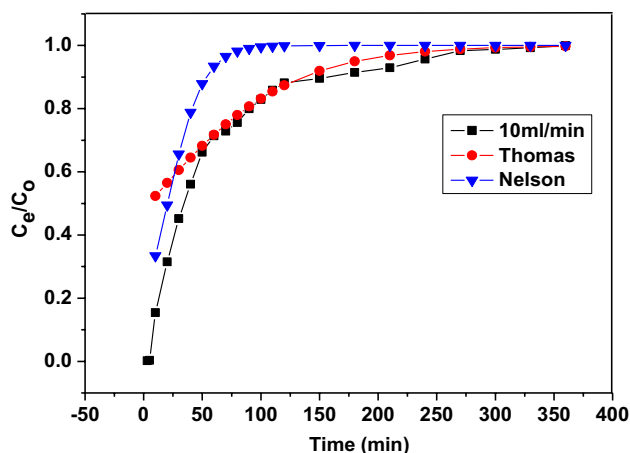


Fig. 8 Breakthrough curves obtained at room temperature for the fixed-bed adsorption of AB 80 onto AFF by experimental results with fittings of different models at experimental condition of  $Q = 10$  ml/min,  $Z = 50$  mm and  $C_0 = 100$  mg/l)

inlet concentration are displayed in Fig. 9. The values of  $k_{Th}$  and  $q_0$  increase as the flow rate and bed height increases. As the inlet initial concentration of AB 80 dye increases, reduction in both  $q_0$  and  $k_{Th}$  values were attained [23]. Based on comparison of the experimental curve and predicted curves obtained, Thomas model demonstrates some good adjustments with adsorption conditions, although provided with poor correlation. Differences were clearly found between the values of adsorption capacity obtained experimentally and calculated with the model. In general, Thomas model is used to describe the biosorption process behavior in fixed-bed column. However, this model comes with some limitations in that the derivation is based on second-order kinetics and suggests that biosorption is not limited by the chemical reaction, but is measured by the mass transfer at the interface [5, 23].

#### 3.4.3 Bed depth service time (BDST) model

Plot of service time,  $t$  (min) versus bed depth,  $Z$  (cm) was used to derive adsorption capacity,  $N_0$  and rate constant,  $k_a$  of BDST model at  $C_i/C_0$  which correspond to 0.60, 0.50 and 0.16 as displayed in Table 4. The adsorption capacity of the bed per unit bed volume,  $N_0$  increases as the  $C_i/C_0$  values increases. The  $R^2$  values obtained from the experimental data, 0.9884, 0.9947 and 0.9689, support the validity of the BDST model for the adsorption of AB 80 dye in column system [21]. These results indicate that the BDST model enables prediction of adsorbent performance at other operating conditions as well.

Table 2 Yoon–Nelson parameters at different conditions using nonlinear regression analysis

$C_0$ (mg/L)	$Q$ (ml/min)	$Z$ (mm)	$k_{YN}$ ( $\text{min}^{-1}$ )	$\zeta$ (mg/L)	$R^2$
50	10	50	0.08	11.84	0.9810
100	10	50	0.07	20.33	0.9811
150	10	50	0.02	28.97	0.9168
200	10	50	0.01	56.16	0.9547
100	5	50	0.05	39.29	0.9596
100	15	50	0.19	12.43	0.9933
100	20	50	1.32	5.73	0.9623
100	10	25	0.09	15.12	0.9601
100	10	100	0.05	31.94	0.9943



**Table 3** Thomas parameters at different conditions using nonlinear regression analysis

Co (mg/L)	Q (ml/min)	Z (mm)	$K_{Th}$ (mlmin <sup>-1</sup> mg <sup>-1</sup> ) (× 10 <sup>-4</sup> )	$q_0$ (mgg <sup>-1</sup> ) (× 10 <sup>2</sup> )	R <sup>2</sup>
50	10	50	3.31	2.368	0.8466
100	10	50	1.29	1.453	0.9116
150	10	50	0.90	1.246	0.9113
200	10	50	0.5	1.199	0.9445
100	5	50	1.06	1.786	0.9928
100	15	50	1.61	2.068	0.8157
100	20	50	2.63	2.563	0.9337
100	10	75	3.70	1.948	0.9601
100	10	100	4.87	2.852	0.9944

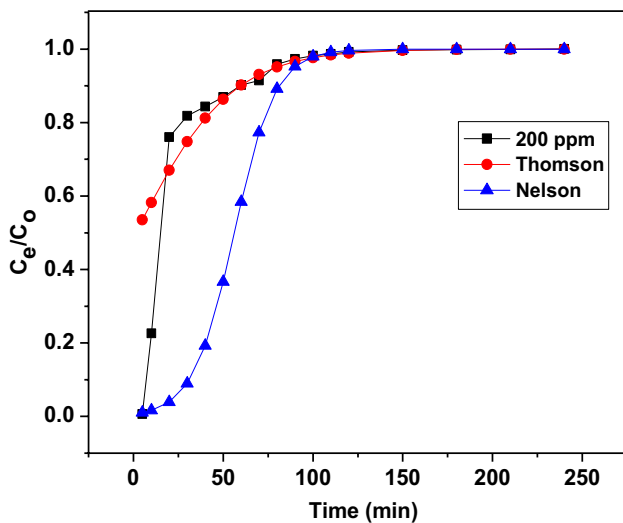


**Fig. 9** Breakthrough curves obtained at room temperature for the fixed-bed adsorption of AB 80 onto AFF by experimental results with fittings of different models at experimental condition of Q= 10 ml/min, Z=50 mm and C<sub>0</sub>=200 mg/l

**Table 4** The calculated constants of BDST model for the adsorption of AB 80 (C<sub>0</sub>= 100 mg/l, Q= 10 ml/min)

$C_i/C_0$	N' (mg/l)	$k_a$ (× 10 <sup>6</sup> ) (l/mg min)	Z (cm)	Service time experimental, t (min)	R <sup>2</sup>
0.16	140.70	671.42	10.0	120	0.9884
0.50	1160.47	7.04	7.5	250	0.9947
0.60	5590.47	- 11.10	5.0	420	0.9689

### 4 Conclusions

In this study, the adsorption performance of AFF onto AB 80 dye was experimented in continuous column mode.

The functionalization of grafted fibers with IMI was verified by characterization with FTIR imaging and SEM analysis. The established biosorbent, AFF was proven as an adsorbent for the removal of AB 80 dyes quite effectively. Column adsorption process parameters such as initial inlet concentration, flow rate and bed height had imposed strong influence onto the adsorption capacity towards AB 80 dye. The results obtained conclude that the dye removal efficiency increases as the bed height increases. Moreover, the total weight of AB 80 dye loaded onto AFF signifies the similar observation too. The AFF capable to accommodate 194.4 mg/g of AB 80 dye particles at flow rate of 5 ml/min, 100 mg/l inlet concentration and 50 mm of bed height. Thomas model defines the behavior of the breakthrough curves well. This experimental outcome recommended that the internal and external diffusion is unreliable to controlling step of the adsorption process in column mode. Validity of the BDST model for the column system which packed with AFF is approved by high values of correlation coefficients (R<sup>2</sup> ~ 0.99) obtained. Conclusively, the experimental data attained for continuous sorption model by using AFF, had proven the efficiency of the AFF as a biosorbent for the removal of dye particles. Therefore, in future AFF is the most suitable to be used as sorbent in natural surrounding for the dye adsorption.

**Acknowledgement** This research was financially supported by Malaysian Nuclear Agency under Ministry Energy, Science, Technology, Environment and Climate Change (MESTECC) (FP0214D052(DSTIN)) received by one of the co-author, N. A. F Othman. The corresponding author also would like to thank Universiti Teknologi Malaysia for giving further financial and consultation assistance under Research University Grant (QJ130000.2546.16H46) awarded to A. K. Zulhairun.

### Compliance with ethical standards

**Conflict of interest** On behalf of all authors, the corresponding author states that there is no conflict of interest.

## References

1. Chowdhury S, Chakraborty S, Saha P (2011) Biosorption of Basic Green 4 from aqueous solution by *Ananas comosus* (pineapple) leaf powder. *Colloid Surf B* 84(2):520–527
2. Bharathi KS, Ramesh SPT (2013) Fixed-bed column studies on biosorption of crystal violet from aqueous solution by *Citrullus lanatus* rind and *Cyperus rotundus*. *Appl Water Sci* 3(4):673–687
3. Şayan E (2006) Optimization and modeling of decolorization and COD reduction of reactive dye solutions by ultrasound-assisted adsorption. *Chem Eng J* 119(2):175–181
4. Ahmad A, Hameed B (2010) Fixed-bed adsorption of reactive azo dye onto granular activated carbon prepared from waste. *J Hazard Mater* 175(1):298–303
5. Han R, Wang Y, Zhao X, Wang Y, Xie F, Cheng B, Tang M (2009) Adsorption of methylene blue by phoenix tree leaf powder in a fixed-bed column: experiments and prediction of breakthrough curves. *Desalination* 245(1–3):284–297
6. Chowdhury S, Saha PD (2013) Artificial neural network (ANN) modeling of adsorption of methylene blue by NaOH-modified rice husk in a fixed-bed column system. *Environ Sci Pollut R* 20(2):1050–1058
7. Liu Y, Kang Y, Huang D, Wang A (2012) Cu<sup>2+</sup> removal from aqueous solution by modified chitosan hydrogels. *J Chem Technol Biotechnol* 87(7):1010–1016
8. Weng C-H, Lin Y-T, Tzeng T-W (2009) Removal of methylene blue from aqueous solution by adsorption onto pineapple leaf powder. *J Hazard Mater* 170(1):417–424
9. Wang J, Chen C (2009) Biosorbents for heavy metals removal and their future. *Biotechnol Adv* 27(2):195–226
10. Selambakkannu\* S, Othman NAF, Mohamad SF, Saidi H (2014) Delignification studies of banana fibers for radiation graft copolymerization. *AJBAS* 8(15):112–118
11. Ma H, Morita K, Hoshina H, Seko N (2011) Synthesis of amine-type adsorbents with emulsion graft polymerization of 4-hydroxybutyl acrylate glycidylether. *Mater Sci Technol* 2(07):776
12. Kumar U, Bandyopadhyay M (2006) Fixed bed column study for Cd(II) removal from wastewater using treated rice husk. *J Hazard Mater* 129(1):253–259
13. Low KS, Lee CK (1991) Removal of metals from electroplating wastes using banana pith. *Bioresour Technol* 38(1):1–6
14. Cheknane B, Baudu M, Basly J-P, Bouras O, Zermane F (2012) Modeling of basic green 4 dynamic sorption onto granular organo-inorgano pillared clays (GOICs) in column reactor. *Chem Eng J* 209:7–12
15. Akar ST, Ari AG, Akar T, Celik S (2011) Decolorization of Reactive Blue 49 contaminated solutions by *Capsicum annum* seeds: batch and continuous mode biosorption applications. *Chem Eng J* 168(1):125–133
16. Futralan CM, Kan CC, Dalida ML, Pascua C, Wan M-W (2011) Fixed-bed column studies on the removal of copper using chitosan immobilized on bentonite. *Carbohydr Polym* 83(2):697–704
17. Chen S, Yue Q, Gao B-Y, Li Q, Xu XZ, Fu K (2012) Adsorption of hexavalent chromium from aqueous solution by modified corn stalk: a fixed-bed column study. *Bioresour Technol* 113:114–120
18. Han R, Wang Y, Zou W, Wang Y, Shi J (2007) Comparison of linear and nonlinear analysis in estimating the Thomas model parameters for methylene blue adsorption onto natural zeolite in fixed-bed column. *J Hazard Mater* 145(1–2):331–335
19. Singh V, Sharma AK, Tripathi DN, Sanghi R (2009) Poly(methylmethacrylate) grafted chitosan: an efficient adsorbent for anionic azo dyes. *J Hazard Mater* 161(2–3):955–966
20. López-Cervantes J, Machado DS, Duarte RGS (2018) Study of a fixed-bed column in the adsorption of an azo dye from an aqueous medium using a chitosan–glutaraldehyde biosorbent. *Adsorpt Sci Technol* 36(1–2):215–232
21. Singha S, Sarkar U (2015) Analysis of the dynamics of a packed column using semi-empirical models: case studies with the removal of hexavalent chromium from effluent wastewater. *Korean J Chem Eng* 32(1):20–29
22. Karimi M, Akbar S, Ali N, Mohammad AJ (2012) Column study of Cr (VI) adsorption onto modified silica–polyacrylamide microspheres composite. *Chem Eng J* 210:280–288
23. Aksu Z, Gönen F (2004) Biosorption of phenol by immobilized activated sludge in a continuous packed bed: prediction of breakthrough curves. *Process Biochem* 39(5):599–613